Results in Physics 11 (2018) 1075–1079

Contents lists available at ScienceDirect

Results in Physics

journal homepage: www.elsevier.com/locate/rinp

Synthesis of α-Al_2O_3 from aluminum cans by wet-chemical methods

Rigoberto López-Juárez[a], Neftalí Razo-Perez[b], Teresita Pérez-Juache[b], Orlando Hernandez-Cristobal[b], Simón Yobanny Reyes-López[c,*]

[a] Unidad Morelia del Instituto de Investigaciones en Materiales, Universidad Nacional Autónoma de México, Antigua Carretera a Pátzcuaro No. 8701, Col. Ex Hacienda de San José de la Huerta, C.P. 58190 Morelia, Michoacán, Mexico
[b] Escuela Nacional de Estudios Superiores, Universidad Nacional Autónoma de México, Antigua Carretera a Pátzcuaro No. 8701, Col. Ex Hacienda de San José de la Huerta, C.P. 58190 Morelia, Michoacán, Mexico
[c] Instituto de Ciencias Biomédicas, Universidad Autónoma de Ciudad Juárez, Envolvente del PRONAF y Estocolmo s/n, C.P. 32310 Ciudad Juárez, Chihuahua, Mexico

ARTICLE INFO

Keywords:
α-Al_2O_3
Aluminum cans
X-ray diffraction

ABSTRACT

Chemical synthesis results in the most convenient route to produce ceramics particles. In this paper, the synthesis of α-Al_2O_3 from aluminum cans is reported. Two approaches were considered for synthesis of α-Al_2O_3, the first route proposed was the precipitation of aluminum chloride with NaOH for producing aluminum hydroxide. The second methodology consist of dissolving aluminum flakes with glacial acetic acid to produce aluminum acetate. The XRD analysis demonstrate that alumina powders are obtained from heat treatment of aluminum acetate at relative low temperature (1100 °C), and at 1180 °C when starting from aluminum hydroxide. The methodology has the capability to produce nanophase alumina powder, the average crystal size was 58–54 nm for alumina derived from hydroxide and aluminum acetate, respectively. Therefore, the use of this precursors simplifies the process and provides another alternative for synthesis of crystalline alumina.

Introduction

α-Alumina is widely employed as substrate in the electronic industry, as support material for catalysis, high temperature crucibles, milling media in high and conventional ball mills, grinding paste for metal polishing, etc. [1]. The high thermal and chemical stability as well as high mechanical strength make possible these diverse applications [1–3]. Alumina is mainly produced industrially by the Bayer process [4–5], which consume a lot of energy. Other methods have been reported for the preparation of alumina, that include precipitation [6], sol-gel [7–8], hydrothermal [9] and other methods [10–11]. Recently, some approaches have been reported for the use of aluminum cans for the synthesis of alumina [3,12–14]. Recycling this type of aluminum waste can save energy and other raw materials [3,14].

On the other hand, independently of the synthesis method or precursors used for synthesis of α-alumina, several phase transformations are observed, the following sequence is commonly reported for most studies: $\gamma \rightarrow \delta \rightarrow \theta \rightarrow \alpha$, [2,13,15]. The required temperature for each phase transformation depends upon the synthesis method and the specific characteristics of precursors [2], but it is common to use temperatures as high as 1200 °C for several hours for the synthesis of the stable α-Al_2O_3, at lower temperatures the δ or θ phases, or both are obtained as the main products. For structural or thermal applications high temperature is used for producing the final ceramic bodies, and at the sintering temperature the α-Al_2O_3 is the stable phase. So, for this applications nanometric α-Al_2O_3 powders are required [15–20].

Chemical synthesis and sol-gel result the most convenient route to produce ceramic particules or nanoparticles. Chemical synthesis is a particularly simple, safe and rapid fabrication process wherein the main advantages are energy and time saving. This quick, straightforward process can be used to synthesize homogeneous, high-purity, crystalline oxide ceramic powders including ultrafine alumina powders with a broad range of particle sizes. The sol-gel method consists in the formation of a sol from organometallic precursors, whose suspended particles polymerize at low temperature. The wet gel generated is then dried and heat treated. Highly pure particles with large surface area can be obtained by sintering ceramic precursors prepared by chemical synthesis and sol-gel methods [21–23].

Several properties of ceramics are influenced by the stability of precursor colloid solution. The main factors which affect stability are ionic strength, surface charges, pH, temperature and addition of dispersant agents. Particle agglomeration can be prevented through dispersant additives. Organic dispersants improve colloid stability and enhance green densification. Also, the temperature required for

* Corresponding author.
E-mail address: simon.reyes@uacj.mx (S.Y. Reyes-López).

https://doi.org/10.1016/j.rinp.2018.11.037
Received 5 September 2018; Received in revised form 11 November 2018; Accepted 11 November 2018
Available online 15 November 2018

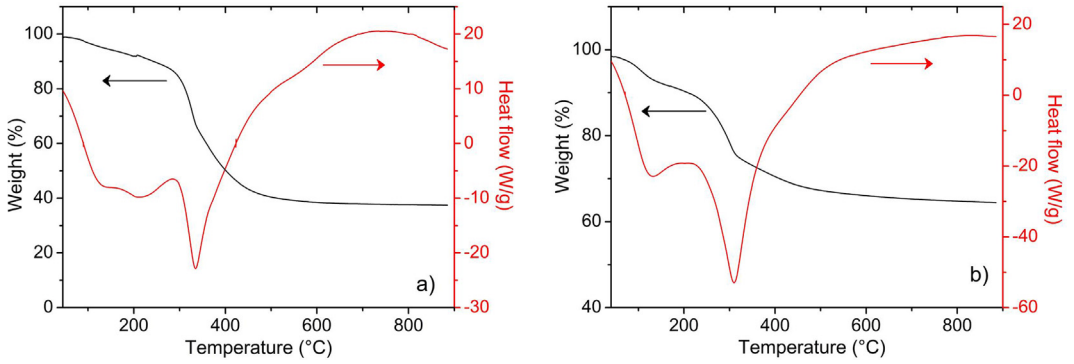

Fig. 1. TG and DCS analysis of (a) aluminum acetate and (b) aluminum hydroxide.

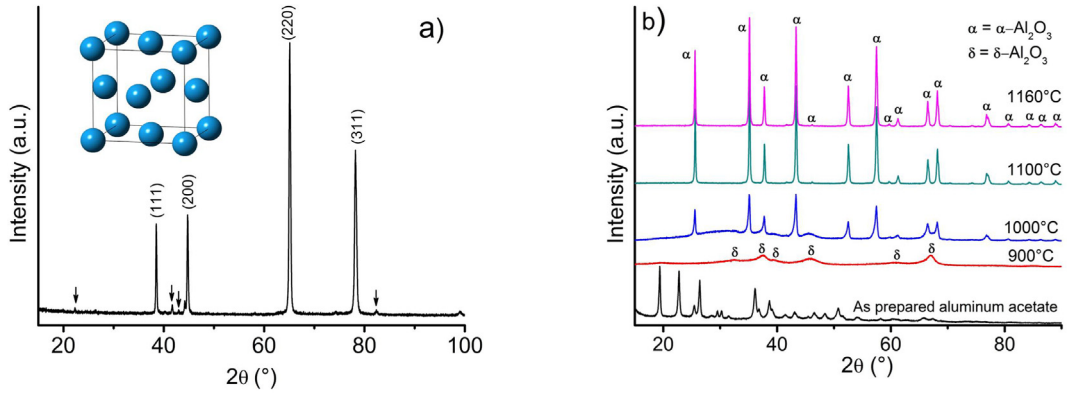

Fig. 2. (a) XRD pattern of a piece of aluminum can, and (b) XRD patterns of aluminum acetate and powders heat treated at different temperatures for 3 h.

sintering process decreases. It has been reported that organic compounds rich in carboxyl and hydroxyl groups are the best option for enhancing particle dispersion [21–24]. Moreover, it is possible to control stoichiometry and morphology, and synthesize materials with required characteristics to suit specific purposes. Therefore, it is necessary to develop more efficient pathways for obtaining alumina nanopowders by chemical synthesis and sol-gel methods. Then, in this paper, the low temperature synthesis of α-Al_2O_3 is reported using aluminum cans as raw material. The methodology represents a viable processing route for recycling aluminum and production of α-Al_2O_3.

Experimental section

Synthesis of powders

For the synthesis of α-alumina powders the raw materials used were aluminum cans, glacial acetic acid (ACS reagent grade, JT Baker), HCl (6 M, Quimica Meyer), NaOH (6 M, Quimica Meyer) and distilled water with electrical conductivity ~3 μS/cm (HI9829 multiparameter, HANNA). First, the aluminum cans were cut into flakes of 2 × 2 cm^2, following by treatment with glacial acetic acid for removing paint and the internal covering polymer. For dissolving aluminum, two approaches were followed: One using HCl and the other with acetic acid. In the HCl process, the aluminum was dissolved into HCl 6 M slowly added for avoiding any risk derived from the produced H_2 [3]. When the aluminum was completely in solution, NaOH 6 M was added dropwise producing aluminum hydroxide. The precipitate was washed several times with distilled water until the electrical conductivity was under 50 μS/cm in the residual water. This was to ensure the complete elimination of residual NaCl resulting from the reaction between $AlCl_3$ and NaOH [3]. The precipitate was then filtered, dried at 90 °C for 24 h and heat treated at several temperatures ranging from 900 to 1160 °C for 1.5–3 h.

In the second methodology, aluminum was dissolved with glacial acetic acid for several days (90–150). This step has similar duration to the reported procedure for preparing alumina from pseudo-boehmite with formic and acetic acid [1]. After the formation of white precipitate, this was centrifuged at 2500 RPM (Centra CL2 Centrifuge, Thermo Scientific) and washed four times for elimination of excess acetic acid. The solid was dried at 90 °C for 24 h and heat treated between 900 and 1160 °C for 3 h.

Thermal analysis

In order to follow up the sequential transformation of precursors with thermal treatments, TGA/DSC analysis (TGA/DSC SDT Q600 equipment, TA Instruments) were performed from room temperature up to 900 °C, with a heating rate of 10 °C/min.

Structural and microstructural characterization

The crystal structure of precursors and calcined powders was determined by X-ray diffraction analysis with a D2-phaser diffractometer (Bruker), using Cu Kα radiation, measurements were acquired from 15 to 90°. Average crystal size was evaluated from the XRD results using the EVA software (Bruker) which uses the Scherrer equation for this purpose. The powders morphology was observed with a JEOL JSM IT300 microscope that was also used for performing the semi-quantitative chemical analysis.

Sinterability of prepared powders

Alumina pellets (13 mm in diameter and 2 mm in thickness) were uniaxially pressed without any binder (Atlas Manual 15 T Hydraulic Press, Specac Inc.), under 300 MPa and sintered at 1650 °C for 2 h in a high temperature furnace (Thermolyne 46100 High Temperature

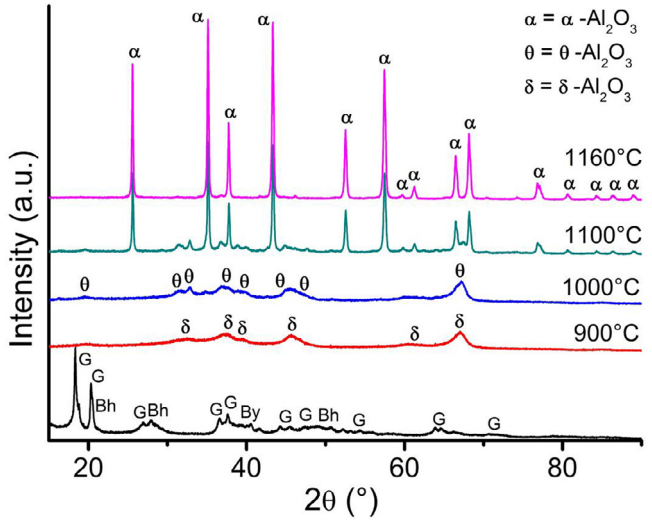

Fig. 3. XRD patterns of aluminum hydroxide and powders heat treated at different temperatures for 3 h (G = Gibbsite, Bh = Bohmite and By = Bayerite).

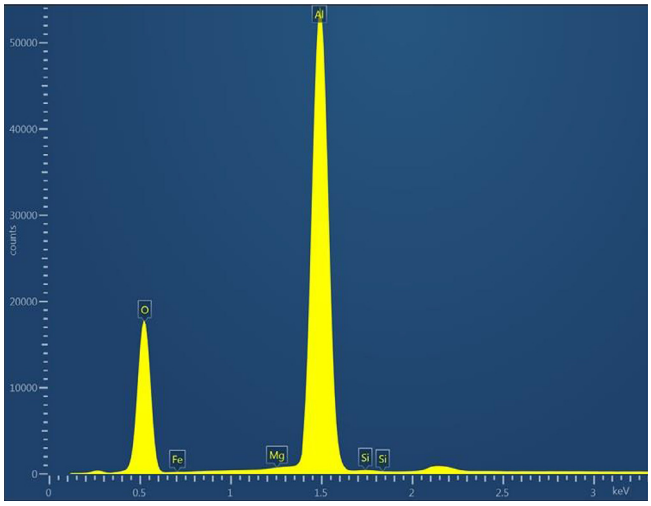

Fig. 5. EDS of ceramics powders at 1160 °C for 3 h.

Table 1
EDS results of ceramics powders at 1160 °C for 3 h.

Element	Atomic % (theoretical)	Atomic % (measured)
O	60	62.70
Mg	–	0.01
Al	40	36.99
Si	–	0.20
Fe	–	0.10
Total	100.00	100.00

furnace). The heating and cooling rates were 5 °C/min and 4 °C/min, respectively. The density of the sintered samples was evaluated by the Archimedes method.

Results and discussion

The TG and DSC results are presented in Fig. 1 for thermal decomposition of aluminum acetate (1a) and aluminum hydroxide (1b). TGA profiles shows a total ceramic yield of 40 and 65 wt% corresponding to the formation of Al_2O_3 from aluminum acetate and aluminum hydroxide, respectively. For the aluminum acetate

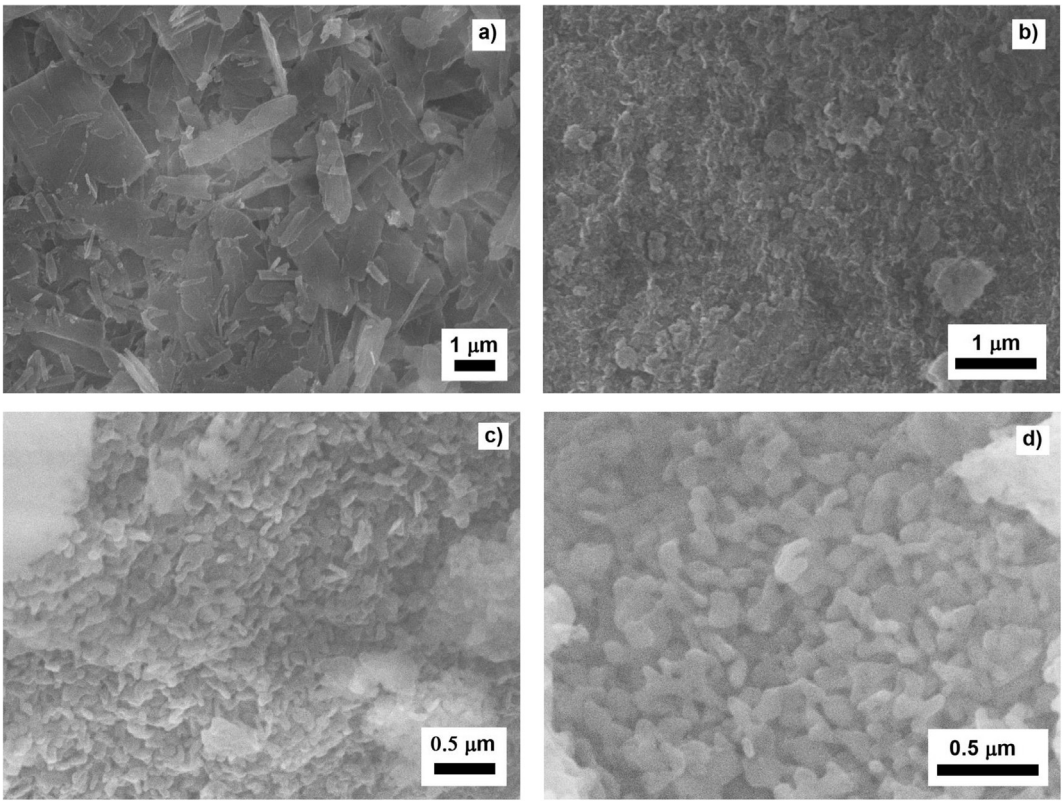

Fig. 4. SEM images of precursors: (a) aluminum acetate, (b) aluminum hydroxide at 1100 °C for 3 h: (c) α-Al_2O_3 from aluminum acetate and (d) α-Al_2O_3 from aluminum hydroxide.

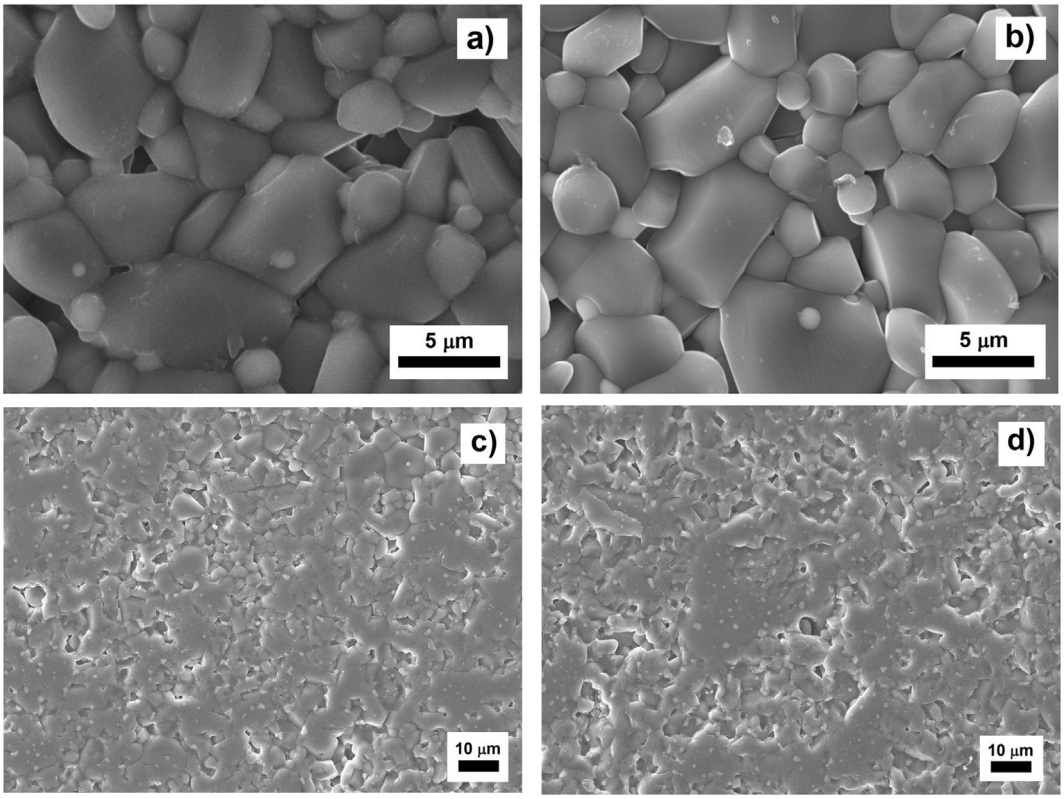

Fig. 6. SEM images of as sintered α-Al_2O_3 prepared from (a) aluminum acetate and (b) from aluminum hydroxide, (c), (d) corresponding polished and thermally etched samples.

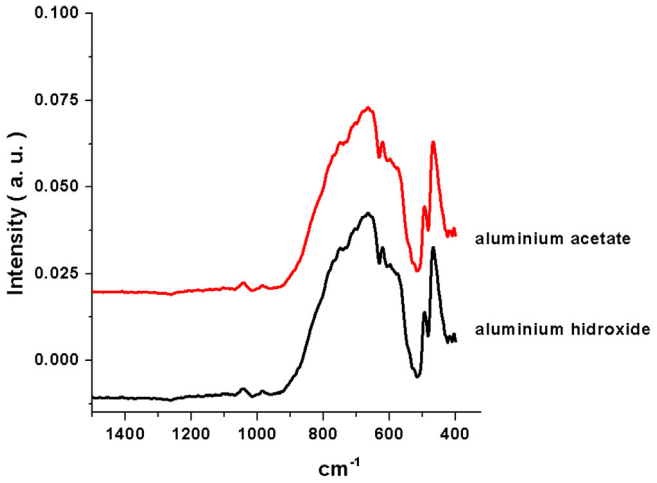

Fig. 7. Infrared spectra of as sintered α-Al_2O_3 prepared from aluminum acetate and aluminum hydroxide.

decomposition, there is a small but continuos loss of mass from room temperature to 300 °C. This could be adscribed to the loss of physically and chemically bonded water. At 325 °C begins the decomposition of aluminum acetate (formation of gamma alumina, not shown in the XRD results), that almost finished at 500 °C which completely agrees with previous studies [1,20–28]. In the heat flow plot, burning of acetate release heat which is clearly observed. More importantly, at 811 °C a small release of energy is observed, which coincide with γ-Al_2O_3 to δ-Al_2O_3 transformation (detected by XRD for sample at 900 °C). Analysing the thermal decomposition of aluminum hydroxide (Fig. 1b), it is clearly seen that between room temperature and 175 °C, the weight loss was related to the physically absorbed water (~7%), while at 200 °C begins the loss of chemically bonded water (dehydration of gibbsite, the main component of the synthesized aluminum hydroxide from cans) which is almost complete at 500 °C. This agrees with previous reports where the final dehydration of boehmite (Al_2O_3-H_2O) to γ-Al_2O_3 takes place close to 450 °C [21–28]. The heat flow coincides perfectly with the events described above. Finally, regarding the thermal decomposition of aluminum acetate and hydroxide. It is worth noting that the total weight loss in aluminum hydroxide is close to 40%, while is ~60% for aluminum acetate. This difference is because during the aluminum acetate heat treatment, a great amount of organic fraction is eliminated. Meanwhile, only physically and chemically linked water is eliminated during heat treatment of aluminum hydroxide. This last result agrees with the XRD analysis, were gibbsite (Al_2O_3-$3H_2O$), boehmite (Al_2O_3-H_2O) and bayerite (a polymorph of gibbsite with the same composition) were identified.

In Fig. 2a the XRD of aluminum cans is observed. As expected, aluminum cans are almost 100% pure as reported in the literature, where manganese, magnesium and iron are the main impurities [14], which represent a total of 2.6%. The impurity (marked with arrows) is assigned to MgO that coincides with the amount of Mg present as impurity in aluminum cans. Analysing the results from the two processes for the synthesis of α-Al_2O_3, for the acetate route, the XRD patterns for aluminum acetate before and after heat treatment at 900–1160 °C are shown in Fig. 2b. The data for aluminum acetate match with the 13–0833 PDF crystallographic card reported before [1]. The powders calcined at 1100 and 1160 °C for 3 h have pure α-Al_2O_3 phase (PDF 04-004-2852). α-Al_2O_3 was obtained at relatively low temperature compared with the recycling process using H_2SO_4 for producing aluminum sulfate [13,16] where 1200 °C for 3 h are needed for synthesis of α-Al_2O_3 pure phase. Furthermore, no toxic gases are produced when acetic acid is used instead of the toxic SO_3 produced after heat treatment of $Al_2(SO_4)_3{\cdot}18H_2O$ Compared with another route for recycling aluminum cans [14], it was reported a lower synthesis temperature (900 °C for 2 h), but magnesium aluminate ($MgAl_2O_4$) spinel impurity

phase was observed. Also, better results are obtained comparing with the synthesis of alumina from acetates and formates which require as high as 1200 °C for synthesis α-Al_2O_3 [1,17]. On the other hand, low temperature synthesis of α-Al_2O_3 was reported using the Pechini [18] and precipitation [19] methods, starting with commercial reagents which represent more expensive and complex routes.

In Fig. 3 the XRD of aluminum hydroxide and heat-treated powders derived from the HCl-NaOH method are shown. The aluminum hydroxide precursor consists of a mixture of Gibbsite (G = Al_2O_3-$3H_2O$), Bohmite (Bh = Al_2O_3-H_2O) and Bayerite (By = Al_2O_3-$3H_2O$, a gibbsite polymorph). Comparing the XRD patterns of powders from both routes, it is clearly seen that in the case of aluminum acetate route, before crystallization of α-Al_2O_3, only δ-Al_2O_3 was obtained. On the other hand, for the HCl-NaOH route, powders at 900 °C only consist of δ-Al_2O_3 phase, meanwhile after heat treatment at 1000 °C a mixture of δ-Al_2O_3 and θ-Al_2O_3 phases was obtained. Finally, after heat treatment at 1160 °C α-Al_2O_3 was the main phase with a small amount o residual θ-Al_2O_3.

The morphology of untreated precursors and heat-treated powders at 1100 °C from both methodologies are observed in Fig. 4. The SEM images of aluminum acetate precursor reveals a flake like morphology with some micrometers of crystal mean size. The aluminum hydroxide consists of smaller crystal agglomerates. It is apparent that this feature influences the final crystal size of calcined samples, as can be seen in Fig. 4c and d. Heat treated powders at 1100 °C for 3 h are agglomerates of submicrometer crystals. From the X-ray results, the measured crystal size was 54 and 58 nm for samples obtained from aluminum acetate and aluminum hydroxide, respectively.

In order to give some insight on the chemical composition of ceramics powders derived from the HCl-NaOH route, EDS analysis was performed on sample at 1160 °C and are shown in Fig. 5 and summarized in Table 1. From the EDS graph, it is clearly seen that most of the X-ray measured correspond to aluminum and oxygen. The measured atomic percentages are very close to the theoretical values, with some impurities, which have been identified in previous studies [22] and completely agree with our results. The measured density for sintered pellets derived from both methods reveals that high density samples are obtained. These values range from 3.87 to 3.91 g/cm^3 which represent 97–98% of theoretical density (3.987 g/cm^3) [27,28].

The SEM images for sintered samples are presented in Fig. 6. The average crystal size determined by ImageJ software was 3.26 and 3.46 μm for sintered samples derived from aluminum acetate and aluminum hydroxide, respectively. Fig. 7 shows IR spectra of Al_2O_3 from aluminum acetate and aluminum hydroxide at 1650 °C for 2 h. Bands corresponding to O—Al—O bonds characteristic of alpha alumina polymorph (octahedral structure AlO_6) are present in the samples at 379, 491, 565 and 633 cm^{-1}.

Conclusions

Synthesis of α-Al_2O_3 was achieved starting from aluminum cans. Crystalline powders were in the order of ~55 nm in average crystal size for both chemical routes. α-Al_2O_3 was obtained at 1100 °C from aluminum acetate, while 1180 °C was required for aluminum hydroxide precursor. The sintered samples reached ~98% of theoretical density, demonstrating the high synterability of produced powders. The methodologies reported in this work are practical approaches for recycling aluminum cans and producing alumina powders.

Acknowledgements

Thanks to PRODEP, Universidad Autónoma de Ciudad Juárez. Special thanks to Criseida Ruiz for TG measurements. R. López-Juárez acknowledges to DGAPA-UNAM for supporting the present work under project PAPIIT-IN101518. The authors also acknowledge to Hector Orozco (UMSNH) for technical assistance.

References

[1] Clar C, Scian AN, Aglietti EF. Synthesis and characterization of aluminum carboxylate gels. Thermochim Acta 2003;407:33–40.
[2] Takht Ravanchi M, Rahimi Fard M, Fereidoon Yaripour SF. Effect of calcination conditions on crystalline structure and pore size distribution for a mesoporous alumina. Chem Eng Commun 2015;202:493–9.
[3] França Adans Y, Rosa Martins A, Estevam Coelho R, Francisco das Virgens C, Daniela Ballarinid A, Santos Carvalho L. A simple way to produce γ-alumina from aluminum cans by precipitation reactions. Mater Res 2016;19:977–82.
[4] Martin ES, Weaver ML. Synthesis and properties of high purity alumina. Am Ceram Soc Bull 1993;72:71–7.
[5] Fujiwara S, Tamura Y, Maki H, Azuma N, Takeuchi Y. Development of new high-purity alumina. Sumitomo Kagaku 2007;1:1–10.
[6] Wang S, Li X, Wang S, Li Y, Zhai Y. Synthesis of γ-alumina via precipitation in ethanol. Mater Lett 2008;62:3552–4.
[7] Rogojan R, Andronescu E, Ghiţulică C, Vasile BS. Shynthesis and characterization of alumina nano-powder obtained by sol-gel method. UPB Sci Bull, Ser B: Chem Mater Sci 2011;73:67–76.
[8] Adraider Y, Hodgson SNB, Sharp MC, Zhang ZY, Nabhani F, Al-Waidh A, et al. Structure characterisation and mechanical properties of crystalline alumina coatings on stainless steel fabricated via sol–gel technology and fibre laser. J Eur Ceram Soc 2012;32:4229–40.
[9] Suchanek WL. Hydrothermal synthesis of alpha alumina (α-Al_2O_3) powders: study of the processing variables and growth mechanisms. J Am Ceram Soc 2010;93:399–412.
[10] Petrakli F, Arkas M, Tsetsekou A. α-Alumina nanospheres from nano-dispersed boehmite synthesized by a wet chemical route. J Am Ceram Soc 2018:1–12. (in press).
[11] Rajendran M, Bhattacharya AK. Low-temperature formation of alpha alumina powders from carboxylate and mixed carboxylate precursors. Mater Lett 1999;39:188–95.
[12] Abood AlSaffar K, Hasan Bdeir LM. Recycling of aluminum beverage cans. J Eng Develop 2008;12:157–63.
[13] Matori KA, Wah LC, Hashim M, Ismail I, Mohd Zaid MH. Phase transformations of α-alumina made from waste aluminum via a precipitation technique. Int J Mol Sci 2012;13:16812–21.
[14] Liu W, Niu T, Yang J, Wang Y, Hu S, Dong Y, et al. Preparation of micron-sized alumina powders from aluminium beverage can by means of sol–gel process. Micro Nano Lett 2011;6:852–4.
[15] Tonejc A, Stubicar M, Tonejc AM. Transformation of AlOOH (boehmite) and Al$(OH)_3$ (gibbsite) to Al_2O_3 (corundum) induced by high energy ball milling. J Mater Sci Lett 1994;13:519–20.
[16] Gonczy ST, Mitsche RT. Process for preparing high purity alpha alumina. U.S. Patent 4615875, 7 October 1986.
[17] Cartaxo JM, Galdino MN, Campos LFA, Ferreira HS, Menezes RR, Neves GA. Synthesis of alumina using aluminum acetate. Mater Sci Forum 2015;805:508–12.
[18] Cava S, Tebcherani SM, Souza IA, Pianaro SA, Paskocimas CA, Longo E, et al. Structural characterization of phase transition of Al_2O_3 nanopowders obtained by polymeric precursor method. Mater Chem Phys 2007;103:394–9.
[19] Su X, Li J. Low temperature synthesis of single-crystal alpha alumina platelets by calcining bayerite and potassium sulfate. J Mater Sci Technol 2011;27:1011–5.
[20] Kiyohara PK, Souza Santos H, Vieira Coelho AC, de Souza Santos P. Structure, surface area and morphology of aluminas from thermal decomposition of Al(OH)$(CH_3COO)_2$ crystals. Anais da Academia Brasileira de Ciências 2000;72:471–95.
[21] Reyes SY, Serrato J, Sugita S. Low-temperature formation of alpha alumina powders via metal organic synthesis. Adv Tech Mat Mat 2006;8:55–62.
[22] Reyes-López SY, Saucedo Acuña R, López Juárez R, Serrato Rodríguez J. Analysis of the phase transformation of aluminum formate $Al(O2CH)_3$ to α-alumina by Raman and infrared spectroscopy. J Ceram Process Res 2013;14(5):627–31.
[23] Roque-Ruiz J, Cabrera-Ontiveros E, González-García G, Reyes-López S. Thermal degradation of aluminum formate sol-gel; synthesis of α-alumina and characterization by ^1H, ^{13}C and ^{27}Al MAS NMR and XRD spectroscopy. Res Phys 2016;7:1096–102.
[24] Patil KC, Aruna ST, Mimani T. Combustion synthesis: an update. Curr Opin Solid State Mater Sci 2002;6:507–12.
[25] Redaoui D, Sahnoune F, Heraiz M, Raghdi A. Mechanism and kinetic parameters of the thermal decomposition of gibbsite $Al(OH)_3$ by thermogravimetric analysis. Acta Phys Pol A 2017;131:562–5.
[26] Tolentino EN, Scanlan CJ, Aboagye AR. High-resolution thermal gravimetric analysis (HI-RES TGA) of bauxites and muds. In: Proceedings of the 9th international alumina quality workshop, 2012 March 18–22, Perth, Australia, p. 219–26.
[27] Yalamaç E, Trapani A, Akkurt S. Sintering and microstructural investigation of gamma-alpha alumina powders. Eng Sci Technol, Int J 2014;17:2–7.
[28] Vargas-Martínez Nadia, de Jesús Ruíz-Baltazar Álvaro, Medellín-Castillo Nahúm A, Reyes-López Simón Yobanny. Synthesis of α-alumina nano-onions by thermal decomposition of aluminum formate. J Nanomater 2018;2018:7. ID 9061378.